

Electron impact dissociation of OCS

W Kedzierski, J Borbely and J W McConkey

Physics Department, University of Windsor, Ontario, Canada N9B 3P4

Received 17 July 2001

Published 5 October 2001

Online at stacks.iop.org/JPhysB/34/4027

Abstract

A special matrix isolation detector, sensitive to $S(^1S_0)$, has been used to study the dissociation of OCS into this fragment over an electron energy range from threshold to 400 eV. The maximum cross section occurs at an impact energy of 55 eV and has been measured to be $3.3 \times 10^{-17} \text{ cm}^2$. Time of flight spectroscopy has been used to monitor fragment kinetic energies. Optically allowed processes are observed to dominate the dissociation. Striking similarities between electron and 157 nm photon dissociation have been noted.

1. Introduction

OCS is a linear triatomic molecule with a permanent dipole moment. It is a minor pollutant in our own atmosphere, where it is believed to play a role in the atmospheric sulfur cycle (Polanyi and Young 1990), and it is known to play a subtle role in the carbon and sulfur chemistries in such astrophysical environments as diffuse and dark interstellar clouds (Van Dishoeck 1998). It is also found as a pollutant in some low-temperature plasmas (Kawada *et al* 2000).

The photoabsorption and photodissociation of OCS have been very widely studied (see, for example, Itakura *et al* (2000), Sugita *et al* (2000), Richter *et al* (1998), Suzuki *et al* (1998), Hikosaka *et al* (1997), Sivakumar *et al* (1988), Tabche-Fouhaile *et al* (1983), Van Veen *et al* (1983), Wu and Judge (1982), Eland and Berkowitz (1979), and references in these). When photodissociation occurs via the first absorption band (210–250 nm), $S(^1D)$ atoms are produced and many studies have been carried out involving further reactions of this species. At somewhat shorter wavelengths, 130–170 nm, the $^1\Sigma^+$ and $^1\Pi$ states become accessible with the dominant production of $S(^1S)$, (see Taylor *et al* (1980), Strauss *et al* (1989), Itakura *et al* (2000), Black and Sharpless (1979), Black *et al* (1980) etc). Between 142 and 160 nm Black *et al* (1975) have measured a quantum yield of close to unity for $S(^1S)$ production.

The C–O bond is much stronger than the C–S one and thus much less work is available on OCS break up via the $O + CS$ channel. Tabche-Fouhaile *et al* (1983) used synchrotron radiation to study the predissociation of OCS Rydberg states and demonstrated that excited CS ($A^1\Pi$) fragments were produced but there does not seem to have been any direct detection of O fragments in the photodissociation studies to date. In general O fragments are considered to be very minor constituents (a few per cent at most) of the overall fragmentation picture.

Electron impact collision studies involving OCS are much more limited. Kawada *et al* (2000) have studied vibrational excitation by electron and positron impact and Sueoka *et al* (1999) measured total cross sections. Kim *et al* (1997) calculated total ionization cross sections for the molecule using their binary-encounter-Bethe (BEB) model and compared their results with unpublished measurements of Srivastava. Flicker *et al* (1978) and Leclerc *et al* (1981) have studied the OCS molecule using high-resolution energy loss spectroscopy. The latter authors had better energy resolution and so were able to identify more features in their spectra. They also presented data over a wider energy loss range (4–17 eV). A feature of the energy loss work is the ability to identify spin forbidden transitions in the electron scattering process. The only previous work on dissociative excitation of OCS by electron impact seems to be by Van Brunt and Mumma (1975). They used time-of-flight (TOF) techniques with Auger type detectors sensitive to metastable states of internal energy greater than approximately 6 eV. They were not able to unambiguously differentiate between the different possible atomic, molecular and Rydberg fragments.

In this work we make use of a special detector which is selectively sensitive to certain metastable particles, in this case to $S(^1S)$ atoms, in order to probe the dissociation channels which give rise to this fragment. This greatly simplifies the analysis of what otherwise would be a very complicated problem.

2. Experimental

The apparatus used in these studies has been described extensively elsewhere (LeClair and McConkey 1993, 1994, Kedzierski *et al* 1998), and so only a brief outline giving the salient features will be included here. A crossed beam apparatus is used in which a pulsed electron beam and the target gas beam are mutually orthogonal. Fragments formed in the interaction drift to a surface detector located in a separate differentially pumped region. The detector consists of a layer of xenon continuously deposited on a cold finger held at 65–69 K. When $O(^1S)$ or $S(^1S)$ atoms impact the Xe surface they thermalize, form excimers and radiate (predominantly a broad band near 725 nm in the case of XeO and a band at somewhat higher wavelength close to 800 nm in the case of XeS). A cooled photomultiplier detects the emission through a suitable filter.

LeClair and McConkey (1993) have described the operation of the matrix detector for the case of $O(^1S)$ based in particular on some earlier work by Lawrence and Apkarian (1992). In the case of $S(^1S)$ it is believed that the operation is similar. The metastable impacts the solid surface, thermalizes and forms an excimer which promptly radiates. Black *et al* (1980) studied the spectral properties of $S(^1S)$ produced by photodissociation of OCS in liquids and observed a broad band close to the atomic ($^1S-^1D$) transition at 772.7 nm. Brom and Lepak (1976) studied the photodissociation of OCS in a solid Ar matrix and observed emission at 755 nm. Taylor *et al* (1980) reported data from a similar study in which OCS was photodissociated in both solid Ar and solid Kr matrices. They used emission bands at 779 nm (Ar) and 789 nm (Kr) as monitors of $S(^1S)$ production. Taylor and Walker (1979a, 1979b) demonstrated that the wavelength of the photoluminescence moves progressively to the red as the rare gas host matrix is changed from Ar to Kr to Xe. In Xe it is peaked at 809 nm. They also measured the lifetime of the XeS radiative emission to be between 2 and 3.5 μs and suggested that the emission is due partly to transitions between loosely bound van der Waals molecular states involving $XeS(^1S)$ and $XeS(^1D)$ and partly to XeS excimer transitions, $XeS(2^1\Sigma^+-1^1\Sigma^+)$ and $XeS(2^1\Sigma^+-1^1\Pi)$. Based on these data we identify our observed emission band (see later), centred at 810 nm, as due to the decay of the excited XeS.

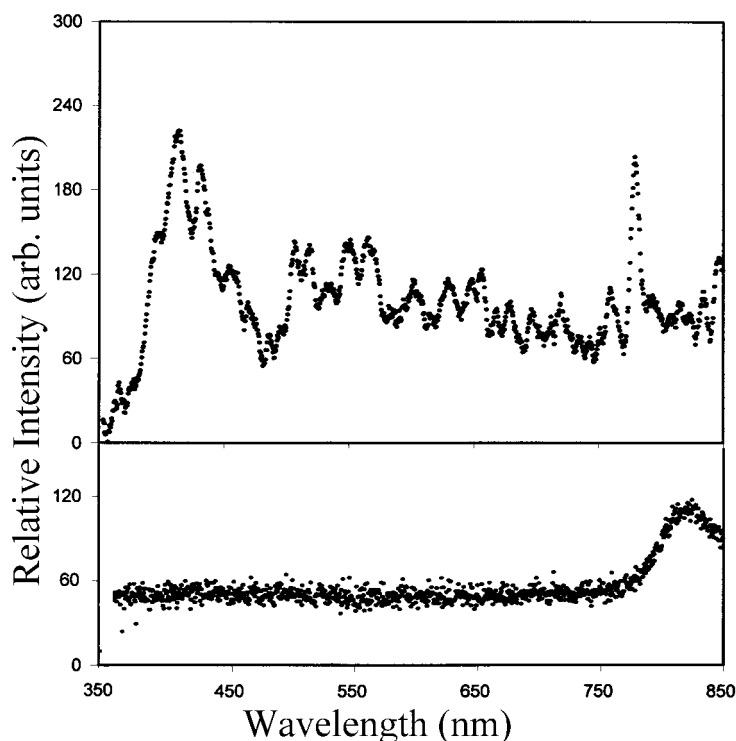


Figure 1. Low-resolution spectra taken at 100 eV electron impact energy. The upper spectrum shows direct fluorescence from the interaction region when the e-beam is on. The lower spectrum shows emission from the cold finger when the e-beam is off. See text for further details.

TOF spectra are acquired at a fixed incident electron beam energy or, alternatively, TOF windows are chosen and excitation functions appropriate to data arriving at the detector during those windows are acquired under computer control. The detector has a high quantum efficiency for O or S(¹S) but is completely insensitive to any other atomic metastables (for example O or S(⁵S)) which are known to be produced in the electron–OCS interaction, see Van Brunt and Mumma (1975)) or other species. The OCS gas had a stated purity of 97.5% and so successive cycles of freezing and thawing were used to pump off any impurities prior to the start of data taking. In order to examine separately the spectral emission from the interaction region and from the cold surface, a low-resolution monochromator was inserted between the photomultiplier and the cold finger and the photomultiplier output was gated either synchronously or non-synchronously with the exciting electron pulse. In this way either the radiation coming directly from the interaction region, or that coming from the cold xenon surface following the arrival of the metastable atoms, could be examined.

3. Results and discussion

In figure 1 we present low-resolution spectral data taken at 100 eV electron impact energy. In the upper part of the figure we show data which are representative of emission directly from the interaction region. At the lower wavelengths the radiation can be identified with various band systems of CO and CO⁺ while at the higher wavelengths the two strong atomic oxygen lines at 777 and 844 nm are prominent. Atomic sulfur emissions at 630 and possibly 566 nm

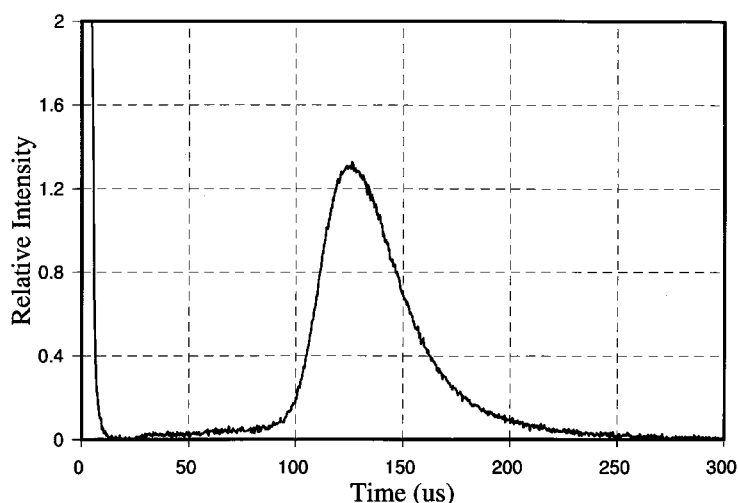


Figure 2. TOF spectrum for metastable $S(^1S)$ fragments produced by 100 eV electron impact on OCS. Zero time corresponds to the centre of the electron pulse.

are also observed. Apart from the sulfur lines, very similar spectra were observed when using CO_2 targets. The lower half of figure 1 shows the spectral distribution of the luminescence from the cold finger under conditions where no direct emission from the interaction region was recorded. A single broad peak with a maximum around 810 nm is evident. This peak may be identified with XeS emission as discussed above. To obtain TOF data a filter was used so that only emissions at wavelengths greater than 650 nm reached the photomultiplier. With this arrangement the dominant prompt radiation recorded was from the strong atomic oxygen lines at 777 and 844 nm.

Figure 2 shows TOF data taken at an incident energy of 100 eV though an essentially identical data set is obtained for all impact energies. The large peak at time zero is due to photons which are produced in the interaction region during the electron beam pulse and which are scattered into the photomultiplier. As such they provide a convenient way of setting the zero of the timescale. A single broad peak is then observed with a maximum at arrival times of 125 μs as the $S(^1S)$ atoms arrive at the xenon surface. Thermalization times at the surface are assumed to be negligible. This is consistent with our findings for $O(^1S)$. The fact that this peak is independent of the incident electron energy is a strong indication that a single $S(^1S)$ production process is dominating the dissociation into this fragment.

Knowing the mass of the detected particle and the distance to the detector it is trivial to convert the TOF data of figure 2 to a kinetic energy spectrum. This is displayed in figure 3 where some smoothing of the data has been applied for clarity. The spectrum is truncated at energies below 0.2 eV because of the poor quality of the data at these low energies. A symmetric peak is observed maximizing at 0.65 eV and with a FWHM of 0.5 eV. This peak in the $S(^1S)$ fragment kinetic energy translates into a total released kinetic energy of 1.4 eV based on conservation of momentum considerations. Assuming that the original transition in the OCS molecule was from the ground $^1\Sigma^+$ to the $2^1\Sigma^+$ excited state where the most probable excitation energy is 8.13 eV (152.3 nm (Rabalais *et al* 1971)), and that 5.87 eV is expended in dissociating OCS into CO and S and in exciting S to the 1S electronic level (see Strauss *et al* (1989)), means that 0.86 eV is available for vibrational and rotational excitation of the CO fragment. This suggests two or three quanta of vibrational excitation of the CO.

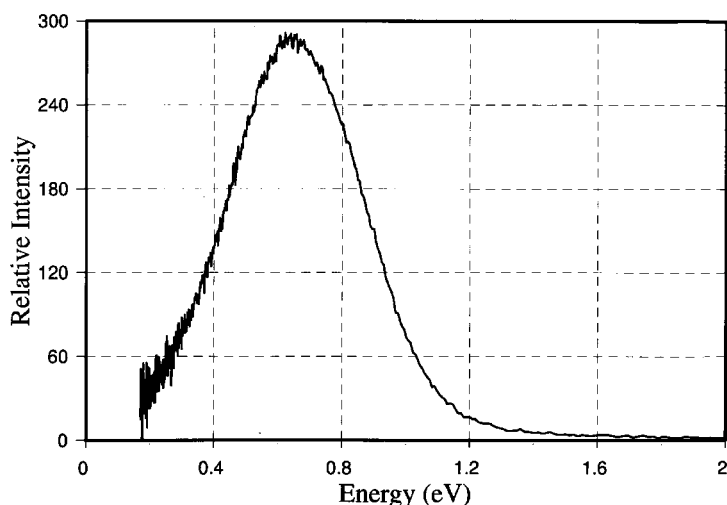


Figure 3. $S(^1S)$ fragment kinetic energy spectrum obtained from the data shown in figure 2.

A number of photodissociation studies of OCS have been carried out, using 157 nm radiation from an F_2 excimer laser, to make direct measurements of the $S(^1S)$ kinetic energy or of the CO vibrational distribution. Ondrey *et al* (1983) deduced a highly inverted CO vibrational population but later measurements by Strauss *et al* (1989) indicated that only vibrational levels $v = 0, 1, 2$ and 3 were significantly populated. Strauss *et al* suggested that the anomalously low translational S atom kinetic energies measured by Ondrey *et al* could have resulted from clustering in the supersonically expanded OCS beam used by these authors. More recent measurements by Itakura *et al* (2000) using Doppler profile analyses to obtain the S atom kinetic energies, are in substantial agreement with the work of Strauss *et al* (1989). Strauss *et al* concluded that about 84% of the energy available to the nuclear motion was allocated to the translational recoil motion of the fragments. This amounts to 1.3 eV in their case. The fact that this agrees well with our average value of 1.4 eV strongly supports our contention that this optically allowed $2^1\Sigma^+$ repulsive state is the major avenue for dissociation via electron impact.

Additional evidence that $S(^1S)$ production is predominantly via dipole allowed channels is obtained from figure 4 which shows the cross section for production of this fragment as a function of impact electron energy. As is evident, the excitation function displays the characteristic broad shape with a maximum near 55 eV. The threshold energy on figure 4 has been set to 8.1 eV based on the discussion above. The absolute cross section scale on figure 4 has been established as follows. Assuming that the $2^1\Sigma^+$ channel dominates we can normalise our measured cross section at high energy to the known optical oscillator strength (0.38, see Ondrey *et al* (1983)), for this transition, using a Bethe–Born procedure similar to that described by LeClair and McConkey (1993). The maximum cross section so obtained is $3.3 \times 10^{-17} \text{ cm}^2$. The error in this procedure depends on the accuracy of the optical oscillator strength and on the accuracy with which the Bethe–Born analysis can be applied (see LeClair and McConkey (1993) for a full discussion of this). Taking these factors into account allows an error estimate of $\pm 10\%$. This measurement may be compared with the maximum cross section for production of $O(^1S)$ from N_2O where a rather similar situation occurs with just one dominant, optically allowed production channel. Here the appropriate oscillator strength was 0.36 and the maximum cross section was $2.25 \times 10^{-17} \text{ cm}^2$ at an impact energy of 45 eV.

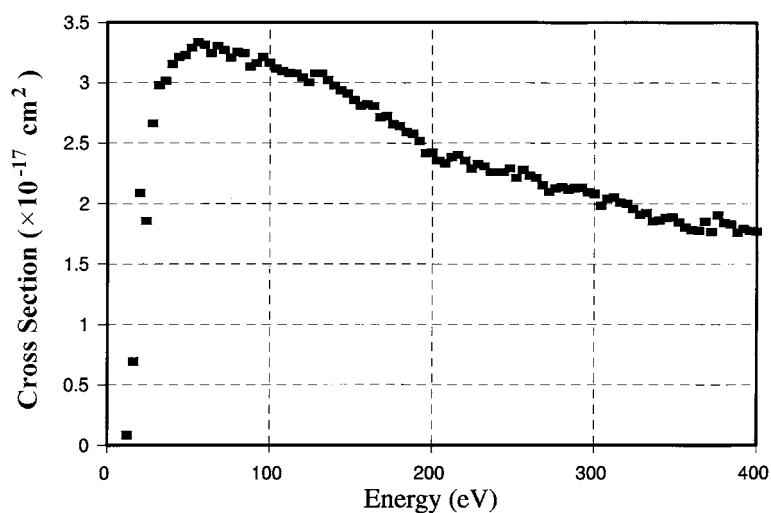


Figure 4. Absolute cross section for production of $S(^1S)$ as a function of incident electron energy. The data have been normalized as discussed in the text.

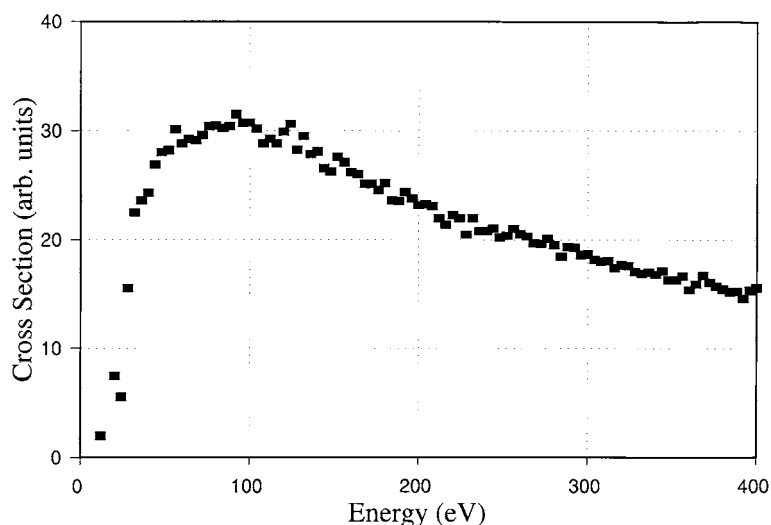


Figure 5. Relative near infra-red emission cross section (mainly 777.4 and 844.7 nm O I transitions) following electron impact on OCS. See text for further details.

Figure 5 shows the relative cross section for production of the prompt infrared photons (mainly 777 and 844 nm O I radiation from dissociative excitation of the parent OCS, see figure 1). Again a rather broad cross section is evident suggesting that here too optical allowed dissociation channels in the parent OCS are dominating the fragmentation. Due to the rather poor statistical accuracy of the data in the near threshold region, it was not possible to measure an accurate appearance energy for the prompt photons. Additional measurements are currently underway to improve this situation as this would help confirm the identification of the source of these prompt photons.

4. Conclusions

The electron impact dissociation of OCS has been studied using TOF spectroscopy and direct detection of the $S(^1S)$ fragment using a solid xenon matrix detector. One dipole allowed dissociation channel is observed to dominate the dissociation and the cross section for this dissociation channel has been measured from threshold to 400 eV. Direct measurements of the fragment energies together with a knowledge of the OCS potential energy curves indicates that the CO(X) molecule, which accompanies the $S(^1S)$, carries two or three vibrational quanta on average. Close similarities with 157 nm photodissociation of OCS have been highlighted.

Acknowledgments

We are grateful to the Natural Sciences and Engineering Research Council of Canada for financial assistance and to the staff of the mechanical and electronic workshops at the University of Windsor for expert technical assistance. Mr Razvan Nistor took some of the preliminary data.

References

- Black G and Sharpless R L 1979 *J. Chem. Phys.* **70** 5571
Black G, Sharpless R L and Lorents D C 1980 *J. Chem. Phys.* **72** 490
Black G, Sharpless R L, Slanger T G and Lorents D C 1975 *J. Chem. Phys.* **62** 4274
Brom J M Jr and Lepak E J 1976 *Chem. Phys. Lett.* **41** 185
Eland J H D and Berkowitz J 1979 *J. Chem. Phys.* **70** 5155
Flicker W M, Mosher O A and Kuppermann A 1978 *J. Chem. Phys.* **69** 3910
Fournier J, Lalo C, Deson J and Vermeil C 1977 *J. Chem. Phys.* **66** 2656
Hikosaka Y, Hattori H, Hikida T and Mitsuki K 1997 *J. Chem. Phys.* **107** 2950
Itakura R, Hishikawa A and Yamanouchi K 2000 *J. Chem. Phys.* **113** 6598
Kawada M K, Sueoka O and Kimura M 2000 *J. Chem. Phys.* **112** 7057
Kedzierski W, Derbyshire J, Malone C and McConkey J W 1998 *J. Phys. B: At. Mol. Opt. Phys.* **31** 5361
Kim Y-K, Hwang W, Weinberger N M, Ali M A and Rudd M E 1997 *J. Chem. Phys.* **106** 1026
Kligler D J, Pummer H, Bischel W K and Rhodes C K 1978 *J. Chem. Phys.* **69** 4652
Lawrence W G and Apkarian V A 1992 *J. Chem. Phys.* **97** 2229
LeClair L R and McConkey J W 1993 *J. Chem. Phys.* **99** 4566
——— 1994 *J. Phys. B: At. Mol. Opt. Phys.* **27** 4039
Leclerc B, Poulin A, Roy D, Hubin-Franskin M J and Delwiche J 1981 *J. Chem. Phys.* **75** 5329
Ondrey G S, Kanfer S and Bersohn R 1983 *J. Chem. Phys.* **79** 179
Polanyi J C and Young P A 1990 *J. Chem. Phys.* **93** 3673
Rabalais J W, McDonald J M, Scherr V and McGlynn S P 1971 *Chem. Rev.* **71** 73
Richter R C, Rosendahl A R, Hynes A J and Lee E P F 1998 *J. Chem. Phys.* **109** 8876
Sivarkumar N, Hall G E, Houston P L, Hepburn J W and Burak I 1988 *J. Chem. Phys.* **88** 3692
Strauss C E, McBane G C, Houston P L, Burak I and Hepburn J W 1989 *J. Chem. Phys.* **90** 5364
Sueoka O, Hamada A, Kimura M, Tanaka H and Kitajama M 1999 *J. Chem. Phys.* **111** 245
Sugita A, Mashino M, Kawasaki M, Matsumi Y, Bershn R, Trott-Kriegeskorte G and Gericke K-H 2000 *J. Chem. Phys.* **112** 7095
Suzuki T, Katayanagi H, Nanbu S and Aoyagi M 1998 *J. Chem. Phys.* **109** 5778
Tabche-Fouhaile A, Hubin-Franskin M-J, Delwiche J P, Frolich H, Ito K, Guyon P-M and Nenner I 1983 *J. Chem. Phys.* **79** 5894
Taylor R V and Walker W C 1979a *J. Chem. Phys.* **70** 284
——— 1979b *Appl. Phys. Lett.* **35** 359
Taylor R V, Walker W C, Monaghan K M and Rehn V 1980 *J. Chem. Phys.* **72** 6743
Van Brunt R J and Mumma M J 1975 *J. Chem. Phys.* **63** 3210
Van Dishoeck E F 1998 *The Molecular Astrophysics of Stars and Galaxies* ed T W Hartquist and D A Williams (New York: Oxford Science)
Van Veen N, Brewer P, Das P and Bersohn R 1983 *J. Chem. Phys.* **79** 4295
Wu C Y R and Judge D L 1982 *J. Chem. Phys.* **76** 2871